

NGC 3067: ADDITIONAL EVIDENCE FOR NONLUMINOUS MATTER?

VERA C. RUBIN,^{a)} NORBERT THONNARD, AND W. KENT FORD, JR.^{a), b)}

Department of Terrestrial Magnetism, Carnegie Institution of Washington, Washington, D.C. 20015

Received 2 October 1981; revised 2 December 1981

ABSTRACT

Optical and 21-cm observations have been made of the small low-luminosity Sb III galaxy NGC 3067. Beyond the nuclear region, rotational velocities rise slowly to 151 km s^{-1} at $R = 7.3 \text{ kpc}$, near the limit of the optical disk. The velocity gradient is $5.2 \text{ km s}^{-1} \text{ kpc}^{-1}$. The absorption previously detected along the line of sight to the QSO 3C 232 is located near the minor axis of NGC 3067 at a projected distance of almost two galactic radii. *If the absorption arises from gas in circular orbit in the plane of NGC 3067*, geometrical considerations require that the rotation velocities continue to rise beyond the optical image, increasing to a velocity near 340 km s^{-1} at $R = 40 \text{ kpc}$. Such a velocity implies that 94% of the mass is located beyond the optical image; this mass has a ratio of M/L_B greater than 100. Observations at 21 cm at Arecibo have not detected hydrogen clouds at this radial distance, but place an upper limit of $10^7 M_\odot$ for the mass of a single cloud.

I. INTRODUCTION

There is now compelling evidence that rotational velocities in spiral galaxies remain constant or increase slowly with increasing radius out to the limits of the optical image, here adopted as R_{25} , the isophotal contour where the surface brightness equals $25 \text{ mag arcsec}^{-2}$. This evidence comes both from 21-cm observations (Bosma 1978) and from optical observations (Rubin *et al.* 1978, 1980) for field spirals. Even for galaxies with neutral hydrogen disks extending well beyond the optical disks, rotational velocities do not fall as is expected for Keplerian mass distributions. These observations imply that significant low-luminosity mass exists at large nuclear distances. They also suggest that knowledge of outer disks of galaxies will be fundamental in understanding the distribution of mass in the universe.

We discuss here possible evidence for mass beyond the optical disk of NGC 3067, an Sb spiral within two arcminutes of a quasar, 3C 232. 3C 232 ($z = 0.513$) is located near the extension of the minor axis of NGC 3067, a galaxy classified Sb (s) III (Sandage and Tamman 1981). Its small complex nuclear structure had earlier led Morgan (1958) to classify it a?I. The separation of the QSO and the galaxy center is $113''.5$ on the sky; the radius of the galaxy is $R_{25} = 74''$. We have obtained spectroscopic and photographic data on NGC 3067 to see if velocity information can put constraints on the disk properties and the mass distribution within the galaxy. A plate of the galaxy/quasar field taken at

the Lowell Observatory 42-in. (1.1 m) telescope is reproduced in Fig. 1. We have also searched for an extended disk of neutral hydrogen several radii beyond the optical disk, and present upper limits on the sizes of gas clouds at very large distances in NGC 3067.

Haschick and Burke (1975) discovered an extremely narrow ($\leq 5.5 \text{ km s}^{-1}$) absorption line of neutral hydrogen at $V = 1418 \pm 2 \text{ km s}^{-1}$ in the spectrum of 3C 232, as well as broad hydrogen emission from NGC 3067. These observations were confirmed by Grewing and Mebold (1975). From high-dispersion optical spectra, Boksenberg and Sargent (1978) discovered the H and K lines of Ca II, at a mean velocity of $1406 \pm 11 \text{ km s}^{-1}$, and a mean FWHM = $90 \pm 15 \text{ km s}^{-1}$. They did not detect the Na I D lines on a single attempt under poor observing conditions. Optical velocities in the inner regions ($r < 30 \text{ arcsec}$) of NGC 3067 were obtained by Danziger and Chromey (1972).

One question posed by these previous observations is where the absorption originates. If a coronal cloud, the cloud is more than 15 kpc from the plane of NGC 3067. This distance is greater than the optical radius of the galaxy, 9.6 kpc ($H = 50 \text{ km s}^{-1} \text{ Mpc}^{-1}$). Furthermore, the narrow line requires that the cloud be cool, in contrast to the wide range of ionization stages detected for the corona of our Galaxy (Savage and deBoer 1981). But if the cloud originates instead in the disk, and is moving in a circular orbit viewed at an inclination of 68° (the inclination of the optical galaxy), then some gas extends at least to 40 kpc, which is over four times the optical radius.

From considerations of column densities, temperatures, velocities, and the absence of Na I, Haschick and Burke, and Boksenberg and Sargent concluded that the absorbing cloud was most likely coronal, rather than disk. However, as these authors recognized, the choice is a difficult one and the evidence for a cool coronal

^{a)}Visiting Astronomer, Kitt Peak National Observatory, which is operated by the Association of Universities for Research in Astronomy, Inc. under contract with the National Science Foundation.

^{b)}Visiting Astronomer, Lowell Observatory.

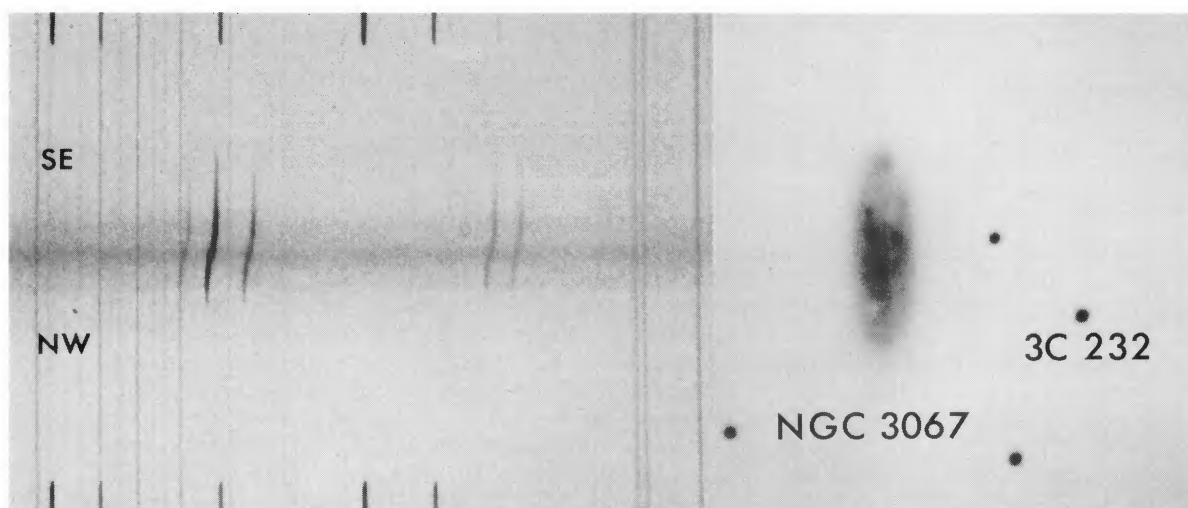


FIG. 1. (left) Spectrum of NGC 3067 taken at the KPNO 4-m RC spectrograph plus image tube, original dispersion = 25 \AA mm^{-1} , exposure time 120 min, position angle = 105° . $H\alpha$, the strongest line, is flanked by [N II] lines; the [S II] doublet is also visible. (right) Reproduction of a plate of NGC 3067 taken at the Lowell Observatory 1.1-m telescope with a Carnegie image tube + BG 23 filter; exposure 30 min. The QSO 3C 232 is indicated.

cloud rather than a disk cloud is not strong. In addition, as Boksenberg *et al.* (1980) point out, there is no reason to expect that the high Na I abundance seen in the inner Galactic disk persists at very large radii. In fact, low Na I values are observed for high-velocity gas in the Galactic plane. Moreover, the C IV line is a valuable marker for halo material. Comparison of its strength in Galactic disk and halo stars indicates that it is formed mainly high in the Galactic halo (Snijders 1980). Its absence (or weakness) in IUE observations of 3C 232 (Boksenberg *et al.* 1981) may strengthen the argument that the absorption comes from disk gas. Additional observations of the Galactic disk absorption (such as that in the direction of 3C 273; Cowie *et al.* 1981), and of 3C 232 (such as the depletion of Na I), might help elucidate the two possibilities.

II. ROTATIONAL VELOCITIES IN NGC 3067

The arguments that we give below depend on derived parameters that are sensitive to the geometry and systemic velocity of the galaxy-QSO pair. These have been determined in several ways and are discussed in the Appendix.

We have determined a rotation curve for NGC 3067, to see what constraints the dynamical information can place on the interpretation of the absorption measures. Velocities come from two spectra of NGC 3067 (Fig. 1, left) with the Kitt Peak 4-m RC spectrograph plus Carnegie image tube (p.a. = 100° and 105° ; major axis = 101.5°). Central velocities of $V_0 = 1458$ and 1454 are measured; we adopt $V_0 = 1456 \pm 5 \text{ km s}^{-1}$ (heliocentric). The rotational velocities shown in Fig. 2 come

from $H\alpha$ and [N II] $\lambda 6383$ lines on each plate, reflected about the central velocity. In the position angles in which we have observed, the emission extends only to $R = 4.0$ kpc NW, but to $R = 7.3$ kpc SE. The rotation curve is smooth and gently rising; from 4.5 to 7.3 kpc the velocities increase linearly at the rate of $5.2 \text{ km s}^{-1} \text{ kpc}^{-1}$.

If we assume that the absorption observed at $V_{\text{abs}} = 1420.0 \pm 0.5 \text{ km s}^{-1}$ (Sec. III) along the line of sight to the QSO arises from a neutral hydrogen cloud orbiting with the circular velocity in the plane of NGC 3067, then we can determine the radial distance and the orbital velocity of the cloud from the velocity difference, $V_0 - V_{\text{abs}} = +36 \pm 5 \text{ km s}^{-1}$. Using the expression (Appendix) for deriving the circular velocity from an off-axis velocity, and the parameters adopted for NGC 3067 (Table I), the radial distance of the absorbing gas is calculated to be $40 (-5, +8) \text{ kpc}$; the rotational velocity is $343 (-65, +100) \text{ km s}^{-1}$. Thus, *if the absorption arises from disk gas in circular orbit*, the rotation curve must continue to rise from its final measured velocity of 151 km s^{-1} at $R = 7.3 \text{ kpc}$ to $V = 343 \text{ km s}^{-1}$ at $R = 40 \text{ kpc}$. It is striking that this velocity is in accord with the velocity predicted ($V = 321 \text{ km s}^{-1}$) if the observed velocity gradient ($4.5\text{--}7.3 \text{ kpc}$) continues to 40 kpc. In Fig. 3 we have indicated on a copy from the Palomar Sky Survey a circular orbit of 40 kpc.

The listed uncertainties come from a consideration of the range of velocities and viewing geometry permitted by the observations. Even though the projection factors are large because the QSO is located 73° from the major axis, the projected velocity still has an acceptable accuracy because of the high accuracy of the 21-cm and optical velocities.

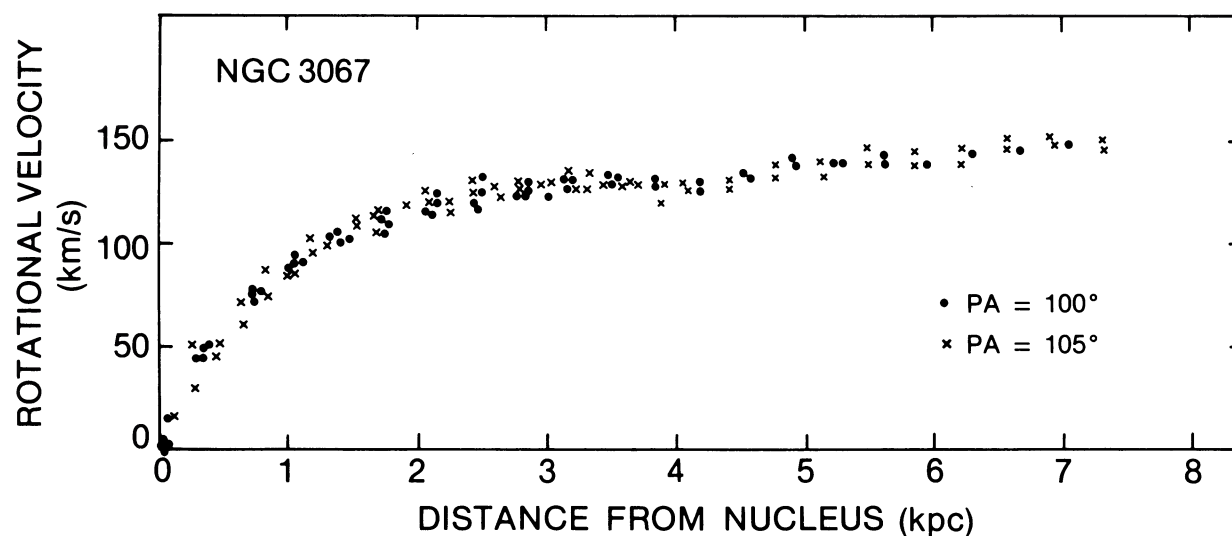


FIG. 2. Rotation velocities in the plane of NGC 3067, as a function of the distance from the center projected to p.a. = $101^{\circ}5$, from H α and [N II] λ 6583 lines. Circles are from spectrum in p.a. = 100° , \times 's are from spectrum in p.a. = 105° .

This (V, R) pair (343 km s^{-1} , 40 kpc) is also consistent with values of (V, R) observed for a sample of Sb galaxies with a wide range of luminosities (Rubin *et al.* 1982). Figure 4 shows this relation between $\log V(R_{25})$ and $\log R_{25}$ for 20 Sb galaxies, and the two locations for NGC 3067. From its optical properties, NGC 3067 is one of the smallest Sb's with a low rotational velocity at R_{25} . Based on the new velocity and radius projected from the absorption feature, NGC 3067 would be among the largest Sb and would have the highest rotational velocity. Note, of course, that the plot is now a hybrid, because the velocity is no longer the R_{25} velocity. However, the new point for NGC 3067 is just in the range for (V, R) values for Sb's of high luminosity. It is hard to know how much importance to give to this circumstance. Is it significant that the projected (V, R) values lie well off the plot of (V, R) values for Sc galaxies, for example?

In summary, these optical observations have added no new evidence as to the location of the cloud seen in absorption around NGC 3067. But they do force an interesting constraint. If the absorbing cloud is in a circular orbit in the plane of the disk, then the rotation curve of NGC 3067 rises slowly at least to 40 kpc , in accord with the velocity gradient seen in the optical disk, and in accord with properties of more luminous, more massive Sb galaxies. The distribution of mass implied by these velocities is discussed in Sec. IV.

III. OBSERVATIONS AT 21 CM

The NGC 3067/3C 232 region was observed at the 21-cm neutral hydrogen line in March 1981 with the

305-m radio telescope of the Arecibo Observatory.* We utilized the dual circularly polarized feed coupled to a cooled GASFET front end yielding a 3.5×3.2 -arcmin beam and a very stable 50-K system temperature at the zenith. The results are summarized in Table II.

We have mapped the neutral hydrogen extent of NGC 3067. The central profile shown in Fig. 5 (center) is of sufficient quality to make meaningful comparisons with the optical spectra. The observed 21-cm velocity extent, measured to the half-power point of each side of the profile, is $1337\text{--}1604 \text{ km s}^{-1}$, in good agreement with the optical ($1336\text{--}1596 \text{ km s}^{-1}$) velocity range. Because of the asymmetry of the hydrogen distribution (discussed below), the midpoint of the H I velocity extent, $1470 \pm 15 \text{ km s}^{-1}$, is biased towards higher velocities. Therefore we adopt the optically derived central velocity. The total integrated flux density is derived from the beam-weighted sum of the central profile, and profiles taken along the major axis offset by ± 1.5 and ± 3.0 arcmin from the nucleus. Because of the small angular size of the galaxy, the first sidelobe of the circular feed does not contribute to the observed signal. Using the adopted distance of 28.3 Mpc , we derive a total H I mass of $1.4 \times 10^9 M_{\odot}$. From the optical rotation curve the mass interior to 9.6 kpc mass is $5.9 \times 10^{10} M_{\odot}$, yielding an H I to dynamical mass ratio of 0.024, typical for Sb galaxies.

*The Arecibo Observatory is a part of the National Astronomy and Ionospheric Center, operated by Cornell University under contract with the National Science Foundation.

TABLE I. Observed and adopted parameters for NGC 3067.

NGC 3067			Source
Central velocity (heliocentric) V_0			
Symmetry of rotation curve	Plate 1739, p.a. = 100° Plate 1735, p.a. = 105°	$1458 \pm 7 \text{ km s}^{-1}$ $1454 \pm 7 \text{ km s}^{-1}$ $1456 \pm 5 \text{ km s}^{-1}$	
Adopted			
Distance ($V_0 + 300 \cos b \sin l / (H = 50 \text{ km s}^{-1} \text{ Mpc}^{-1})$)		28.3 Mpc	
Inclination		$68^\circ (-3^\circ, +4^\circ)$	1
Radius R_{25} (corrected for extinction and inclination)		9.6 kpc	1
Major axis		101.5 ± 1.0	
Velocity range observed	$R = 7.3 \text{ kpc SE}$ $R = 4.0 \text{ kpc NW}$	$V = 1596 \text{ km s}^{-1}$ $V = 1336 \text{ km s}^{-1}$	
Velocity gradient, $4.5 < R < 7.3 \text{ kpc}$		$5.2 \pm 0.7 \text{ km s}^{-1} \text{ kpc}^{-1}$	
3C 232			
Line-of-sight absorption velocity	21 cm 21 cm H and K	$1418 \pm 2 \text{ km s}^{-1}$ $1420 \pm 0.5 \text{ km s}^{-1}$ $1406 \pm 11 \text{ km s}^{-1}$	2 3
Adopted		$1420 \pm 0.5 \text{ km s}^{-1}$	
NGC 3067/3C 232			
ΔR on plane of sky		113.5	
$\Delta \eta$ on plane of sky		73.1 ± 1.0	
$\Delta V (V_{0(3067)} - V_{(3C\ 232)})$		$36 \pm 5 \text{ km s}^{-1}$	
Radius in disk producing absorption		$40 (-5, +8) \text{ kpc}$	
Rotational velocity in plane of disk from deprojection of ΔV		$343 (-65, +100) \text{ km s}^{-1}$	
from extrapolation of velocity gradient to $R = 40 \text{ kpc}$		321 km s^{-1}	
Mass to final observed velocity ($R = 7.3 \text{ kpc}$)		$3.8 \times 10^{10} M_\odot$	
Mass within R_{25} ($R_{25} = 9.6 \text{ kpc}$)		$5.9 \times 10^{10} M_\odot$	
Mass ($9.6 \leq R \leq 40 \text{ kpc}$)		$102 \times 10^{10} M_\odot$	
\int Luminosity ($R < 9.6 \text{ kpc}$) corrected for i and b		$1.7 \times 10^{10} L_\odot$	
\int Luminosity ($9.6 \leq R \leq 40 \text{ kpc}$), assuming surface brightness $\geq 25.5 \text{ mag arcsec}^{-2}$		$\leq 8 \times 10^9 L_\odot$	
M/L_B ($R \leq R_{25}$, i.e., optical image)		3.5 solar units	
M/L_B ($9.6 \leq R \leq 40 \text{ kpc}$)		$\geq 100 \text{ solar units}$	

Source key to Table I

1. de Vaucouleurs *et al.* (1976).
2. Haschick and Burke (1975).
3. Boksenberg and Sargent (1978).

In spite of the limited resolution of the 21-cm map (2.5×1.0 -arcmin galaxy observed with a 3.5×3.2 -arcmin beam), we are able to deduce a few facts about the H I distribution in NGC 3067. The magnitude of the decrease in observed H I signal for the observations displaced from the center indicates that the neutral hydrogen extent of NGC 3067 is not larger than the optical radius. However, the gas seems to be distributed asymmetrically with approximately twice as much H I in the SE (high-velocity) side than in the NW side. We note that the extent of the optical emission (Fig. 1) is also asymmetric, with the ionized gas measureable to nearly twice the radial distance along the SE side of the major axis than along the NW. Asymmetries in the H I profiles are not particularly unusual and generally show a good correlation with both intensity and velocity asymmetries in the optical spectra (Thonnard *et al.* 1982).

If the rotation curve continues rising to 40 kpc, and there is detectable neutral hydrogen at that distance, it

would be possible to unambiguously detect it, in spite of the limited spatial resolution. Because the observed radial velocities along the major axis arising from gas beyond the optical image would be displaced as much as 160 km s^{-1} from the velocities observed within the optical image, the strong H I central signal would not contaminate the spectrum at the velocities expected for gas at large radii. We observed for a total of 175 min at four positions approximately 35 kpc from the center of NGC 3067. To improve the baselines and signal-to-noise, the observations were positioned so that 3C 232 fell in the first null of the Arecibo beam. The two observations 3'5 west of the galaxy were summed (weighted by their rms noise) separately from the two observations 3'1 east; the resulting composite beams are indicated in Fig. 3. These spectra, smoothed to a resolution of 42 km s^{-1} , are shown in the upper and lower pannels of Fig. 5. The weak 3-MJy signals seen between 1300 and 1630 km s^{-1} are due to the residual off-axis response of the telescope

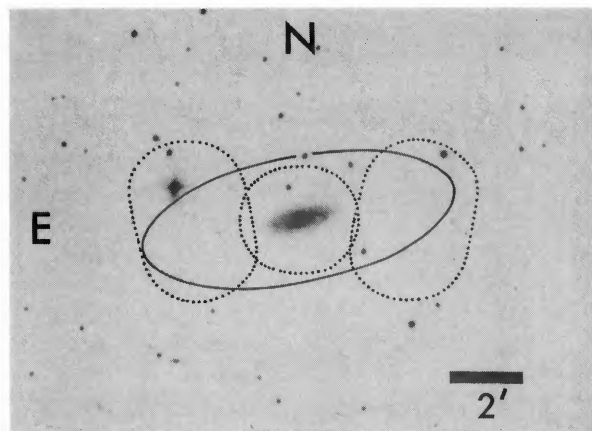


FIG. 3. The NGC 3067 region reproduced from the blue print of the Palomar Sky Survey (copyright 1957, National Geographic-Palomar Observatory Sky Survey). Solid ellipse indicates a 40-kpc circular orbit passing through the projected position of 3C 232. The half-power beam of the 21-cm observations at the central position on the galaxy and the 3.5 W and 3.1 E positions are indicated by dotted lines.

main beam and sidelobes to the H I within the optical image. The hatched regions on either side indicate the velocity range in which disk gas would be found if it extended out to the projected distance of the QSO and the rotation curve continued rising as suggested by the absorption velocity. Signals in these regions give an upper limit of $2.6 \times 10^7 M_\odot$, or less than 2% of the gas in the galaxy. For uniformly distributed gas, this corresponds to a column density of $3 \times 10^{18} \text{ H cm}^{-2}$. While a single $10^7 M_\odot$ cloud of 50-km s^{-1} velocity width could have been detected, this is still 20–40 times more massive than the largest known clouds found around our own galaxy. Therefore, even though we have not found H I at velocities predicted by a rotation curve rising to 40 kpc, the observations cannot rule out a few moderate-size clouds in that region.

The neutral hydrogen absorption feature seen in the direction of 3C 232 was observed at high resolution for a total of 60 min with channel spacings of 0.26 and 0.52 km s^{-1} . The combined spectrum (Fig. 6), smoothed to an effective resolution of 1 km s^{-1} , confirms the observations of Haschick and Burke (1975) and Grewing and Mebold (1975) and also offers some refinements in the observed parameters. With our improved signal-to-noise, spatial, and velocity resolution, we can rule out any possibility that the absorption feature is not at the position of the QSO. We resolve the shape of the absorption feature, with a hint, visible in both the 0.26- and 0.52-km s^{-1} resolution data, that it may have more than one component. The observed half-width of 3.7 km s^{-1} gives a spin temperature of 300 K, which becomes less than 100 K if the absorption profile is multiple. Integrating the absorption profile, the ratio of column density to spin temperature is $1.1 \times 10^{17} \text{ H cm}^{-2} \text{ K}^{-1}$. The column density is therefore 3×10^{19} or $\leq 1 \times 10^{19} \text{ H cm}^{-2}$, depending on whether or not the absorption line is single or multiple. These values are typical for the high-velocity clouds near the Galaxy (Dieter 1969; Giovanelli 1980). The properties of the absorption profile therefore rule out diffuse, high-temperature halo gas, but unfortunately cannot distinguish between an H I cloud in the outer disk of NGC 3067 or a cloud similar to the high-velocity clouds seen at intermediate or high galactic latitudes.

IV. DISCUSSION AND CONCLUSIONS

It is not possible to determine unambiguously with the available information whether the absorbing cloud seen along the line of sight to 3C 232 arises in a halo or in the disk of NGC 3067. If the absorption arises from a cloud in a rotating or nonrotating halo, then the geometry is too indefinite to permit meaningful conclusions. Note, however, that the cloud velocity is negative with respect to the nucleus, as are the rotational velocities on that half of the galaxy. Even if the cloud is located in the disk, the presence of warps at large radial distances, or

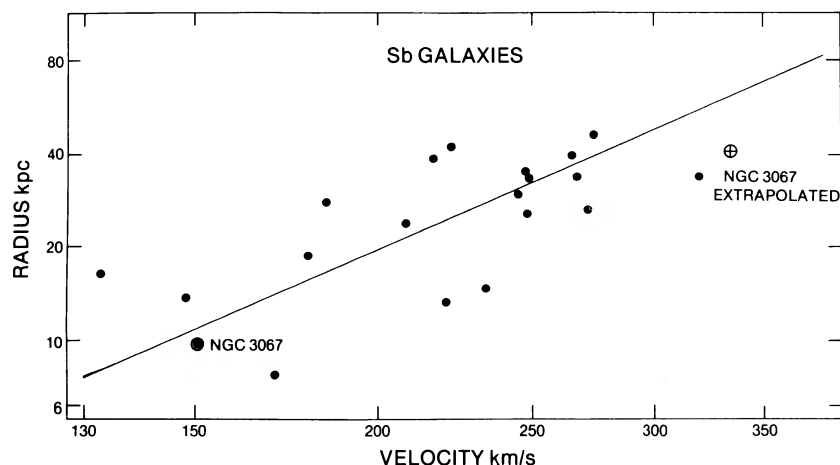


FIG. 4. The correlation of isophotal radius R_{25} with final velocity $V(R_{25})$ for 20 Sb galaxies. NGC 3067 (Sb III) is a small, low-luminosity, low-rotational-velocity member of the set. The velocity and radius implied by the absorption along the line of sight to 3C 232 would place NGC 3067 at the upper end of the relation.

TABLE II. Neutral hydrogen observations in the NGC 3067 region.

NGC 3067		
From central profile:		
R.A.		9 ^h 55 ^m 26 ^s 0
Dec.		+ 32°36'30"
Velocity extent		1337–1604 km s ⁻¹
Central velocity		1470 ± 15 km s ⁻¹
Integrated H I flux density:		
Central profile		6.14 Jy km s ⁻¹
1'5 NW		4.08 Jy km s ⁻¹
1'5 SE		5.65 Jy km s ⁻¹
3'0 NW		0.88 Jy km s ⁻¹
3'0 SE		0.82 Jy km s ⁻¹
From beam-weight sum:		
total integrated H I flux density		7.5 ± 1.0 Jy km s ⁻¹
H I mass		1.4 × 10 ⁹ M _⊙
Search for weak H I at large radius		
identification	3'5 W	3'1 E
R.A.	9 ^h 55 ^m 9 ^s 8	9 ^h 55 ^m 40 ^s 8
Dec.	+ 32°36'27"	+ 32°36'40"
radial distance from center	36	32 kpc
rms per channel	0.28	0.31 mJy
expected velocity range	1000–1275	1645–1920 km s ⁻¹
integrated H I flux density	≤ 0.14	≤ 0.14 Jy km s ⁻¹
H I mass	≤ 2.6 × 10 ⁷	≤ 2.6 × 10 ⁷ M _⊙
3C 232		
R.A.		9 ^h 55 ^m 25 ^s 4
Dec.		+ 32°38'23"
Continuum antenna temperature		12.6 ± 1.5 K
Central velocity of H I absorption		1420.0 ± 0.5 km s ⁻¹
Half-power width of absorption		3.7 ± 0.2 km s ⁻¹
Peak optical depth (τ)		0.027 ± 0.0018
∫ τ(v) dv		0.211 km s ⁻¹

anomalous or streaming motions can distort the analysis. If, however, we make the simplest assumption that the cloud is moving in the plane of the disk with a circular orbit, then these observations have interesting implications for the distribution of nonluminous mass in disk galaxies.

Assume that the cloud is in the disk, hence at 40 kpc. The cloud feels a total dynamical mass (assumed spherical) of $1.0 \times 10^{12} M_{\odot}$; only 6% of this ($5.9 \times 10^{10} M_{\odot}$) is contained within the optical image, $R \leq 9.6$ kpc. The luminosity of the optical image is $1.7 \times 10^{10} L_{\odot}$; the ratio of the dynamical mass to the blue optical luminosity ($R \leq 9.6$ kpc) is 3.5. This low value of M/L_B (i.e., the ratio of the dynamical mass contained within the isophotal radius to the optical luminosity) is consistent with values of M/L_B for other Sb and Sc galaxies which we have studied.

We can calculate the value of M/L_B for the range $9.6 < R \leq 40$ kpc. The surface brightness in this region must be below 25 mag arcsec⁻² so as to be undetectable on the Palomar Sky Survey. This implies a luminosity

less than $8 \times 10^9 L_{\odot}$ if the disk is of constant surface brightness of 25^m5. Thus, over 94% of the mass, but less than 30% of the luminosity, comes from the region beyond the optical disk but within the radial distance of the absorbing cloud. These values require that the ratio of the dynamical mass to optical luminosity average to a value greater than 100 beyond the optical galaxy. This is an extreme lower limit for M/L_B , for it is more likely that the disk surface brightness continues to decrease with increasing radius.

If this interpretation is correct, then in NGC 3067 we are detecting by its gravitational force on an outlying hydrogen cloud a low-luminosity component of mass. This mass is located principally beyond the optical image. Such a circumstance has been predicted earlier, to stabilize disk galaxies and to produce flat rotation curves. Additional studies of the astrophysical properties of the disk and halo of our Galaxy may ultimately tell us if the properties of the absorption produced by the NGC 3067 cloud are consistent with a disk environment. Otherwise, it may take a statistical analysis of ad-

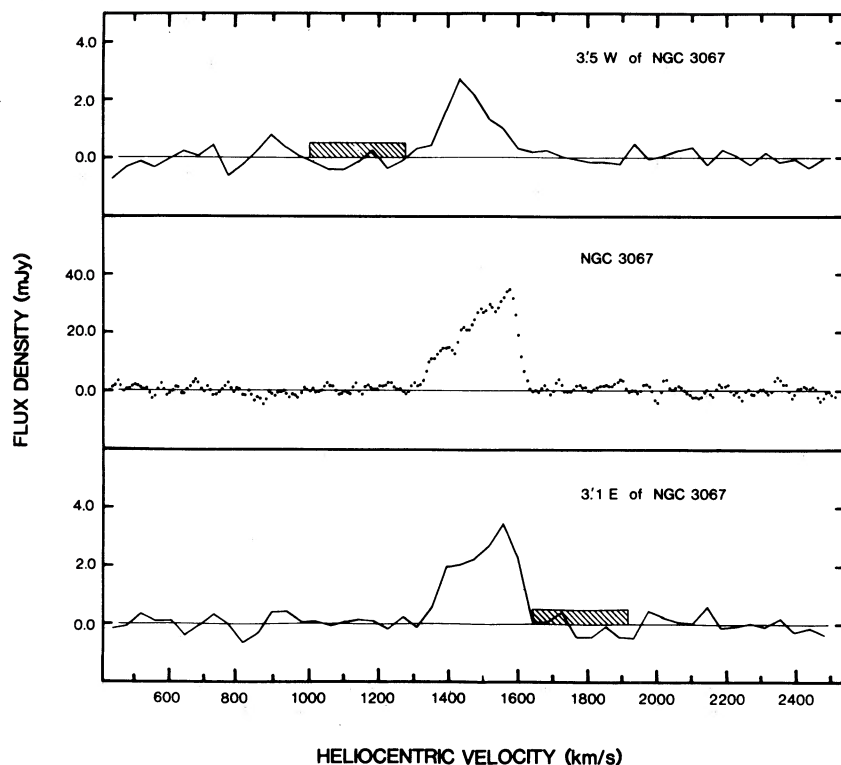


FIG. 5. (center) 21-cm velocity profile at the central position in NGC 3067. Resolution after Hanning smoothing is 16 km s^{-1} . (top and bottom) 21-cm observations 3.5 W and 3.1 E of NGC 3067. Note the flux scale is one-tenth that of central panel; velocity resolution is 42 km s^{-1} . Signal seen between 1300 and 1650 km s^{-1} is due to residual response of telescope main beam and sidelobes to neutral hydrogen in the galaxy. Hatched areas delineate velocities at which a signal would be expected if the rotation curve continued rising and sufficient H I was present at large radii in the disk.

ditional cases like NGC 3067/3C 232 to see if all such cases indicate rotation curves which continue to rise beyond the limits of the optical galaxies.

We are indebted to the Directors and support staffs of Arecibo Observatory, Kitt Peak National Observatory, and Lowell Observatory for observing time and assistance. V.R. thanks the Department of Astronomy, University of California at Berkeley, for the award of a Chancellor's Distinguished Professorship, during which much of this analysis was carried out. We also

thank Dr. Bruce Elmegreen, Dr. Riccardo Giovanelli, Dr. Martha Haynes, and Dr. Don York for helpful conversations and assistance, and a skeptical referee who forced us to reconsider the geometry with great care.

APPENDIX

Because the line joining the center of NGC 3067 with 3C 232 is close to the minor axis of the galaxy, the deprojected radii and velocities are very sensitive to the geometry and measured radial velocities of the system. Many

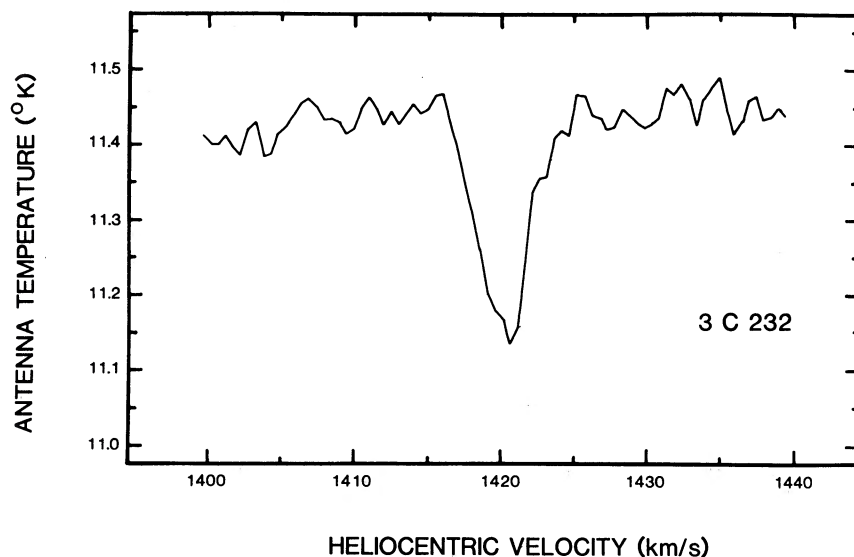


FIG. 6. 21-cm absorption profile seen in the direction of 3C 232. The velocity resolution after smoothing is 1 km s^{-1} .

of the quoted values in the literature are of insufficient precision to be useful. We have redetermined these quantities with care and compare them to published values where available.

To determine rotational velocities and radii in the plane of the galaxy, we use the following expressions. For a galaxy inclined by an angle i to the line of sight ($i = 0$ is face-on) and a point p at a projected distance s from the center with angle η from the major axis, then, assuming p is in the plane of the galaxy, the radial distance R is

$$R = sf(i, \eta),$$

and the rotational velocity V_{rot} is

$$V_{\text{rot}} = (V_p - V_{\text{sys}})f(i, \eta)/\sin i \cos \eta,$$

where

$$f(i, \eta) = (\sec^2 i - \tan^2 i \cos^2 \eta)^{1/2},$$

V_p is the observed radial velocity at p , and V_{sys} is the systemic velocity of the galaxy.

a) Velocities

The absorption velocity at the position of 3C 232, $V_p = 1420.0 \pm 0.5 \text{ km s}^{-1}$, is very well determined from the 21-cm observations.

The optical velocities of NGC 3067 were derived from two high-dispersion spectra (25 Å mm^{-1}) taken on different days. The H α and [N II] λ 6583 lines were measured relative to a new determination (Brault and Hubbard 1981, private communication) of the OH night-sky lines. From each spectrum the central velocity was determined by (1) averaging the observed radial velocity on each side of the major axis over several radius intervals and using the mean, and (2) minimizing the scatter between the measured points and these same points rotated 180° about the nucleus. The above approach assumes dynamical symmetry on the oncoming and receding halves of the galaxy, which is the case for NGC 3067. For the spectrum taken at p.a. = 100° , (1) gives $V_0 = 1458.0 \pm 1.8 (1\sigma) \text{ km s}^{-1}$, (2) gives $V_0 = 1458.4 \pm 1.3$. For the spectrum at p.a. = 105° , (1) gives 1453.2 ± 1.4 and (2) gives 1453.9 ± 1.8 . We adopt $V_0 = 1456 \pm 5 \text{ km s}^{-1}$.

At 21-cm we have five observations along the major axis of NGC 3067. Owing to poor signal-to-noise in two of the mapped points, the combined integrated profile has twice the rms of the central profile; we therefore adopt the central profile for velocity measurements. (We note that owing to the small angular size of the galaxy, the central profile shape and measured velocities are virtually identical to those of the combined profile). Measuring the velocity at half-power of the low-velocity peak of the profile, and at half-power of the high-velocity peak, gives the velocity extent of the galaxy at 21-cm. The central velocity is defined as the midpoint of the two. For 26 Sc and Sb galaxies having high-quality optical and 21-cm observations, the above procedures pro-

duce the best match between optical and 21-cm central velocity and velocity extent: $\Delta V_0(\text{opt} - 21) = 0.23 \pm 7.5 (1\sigma) \text{ km s}^{-1}$ (Thonnard *et al.* 1982). There is however, a fundamental difference between the determination of the optical and 21-cm central velocities. The optical spectrum spatially resolves velocities along the major axis. Therefore, even if H α emission extends much farther on one side of the galaxy than the other, the central velocity is still well determined from symmetry considerations. But if no detectable neutral hydrogen exists at large radii on one side of the galaxy, and the rotation curve is still rising at that radius, then the midpoint of the 21-cm velocity extent is not the systemic velocity.

From the excellent agreement between the optical and 21-cm velocity extent (Tables I and II) we conclude that there are no systematic zero-point differences in the velocities. The much smaller radial H α extent on the NW (low-velocity) side of the galaxy (Fig. 1), the lower integrated H I flux density (Table II), and the asymmetry of the 21-cm profile all indicate that the NW side of the galaxy is gas deficient. This biases the 21-cm central profile to higher values. Hence, we adopt the optical velocity as the systemic for NGC 3067.

b) Inclination

Given an isophotal axial ratio a/b , we can calculate the inclination i of a late-type (Sb or Sc) spiral galaxy with

$$i = \cos^{-1}(1.042b^2/a^2 - 0.042)^{1/2},$$

where the extra terms account for the finite thickness of the disk. In an attempt to determine limits to the inclination of NGC 3067, we have traced transparencies copied from the blue and red prints of the Palomar Observatory Sky Survey and compared them to published values. The results are listed below:

68:1 RC2, de Vaucouleurs *et al.* (1976);

72:0 UGC, Nilson (1973);

69:2 Danziger and Chromey (1972);

67:1 POSS blue, outermost extremity;

69:8 POSS red, outermost extremity.

Measurements taken to brighter levels in the galaxy, such as the image-tube plate (Fig. 1) and higher levels on the POSS copies give inclinations ranging from 71.4 to 73.9 . These are probably less reliable owing to the complicated morphology of the galaxy. We therefore adopt the RC2 value of 68° and assign errors of -3° , $+4^\circ$.

c) Position Angle of the Major Axis

Danziger and Chromey (1972) have spectroscopic observations at several position angles extending over the inner 10–30 arcsec of NGC 3067. Unfortunately their data are at low dispersion and have zero-point velocity errors between spectra, which make a dynamical solution for the major axis unreliable. From photographs, they estimate the major axis at p.a. = 106° . The UGC

lists the major axis at p.a. = 105° . We have spectroscopic observations at p.a. = 105° and p.a. = 100° . In the region over which both sides of the galaxy show emission, the p.a. = 100° rotational velocities are consistently slightly higher, indicating that the major axis is definitely not 105° , but in fact closer to 100° . The best fit to the spectroscopic data is p.a. = 101.5° . Measurements of the major axis from symmetry of the image on enlargements of the POSS blue and red prints, referred to SAO stars, yielded 101.5° and 102.8° , respectively. We adopt p.a. = $101.5^\circ \pm 1.0^\circ$.

d) Position Angle and Projected Distance to the QSO

Measurements (referred to the same SAO stars used

above) on the enlargements of the POSS blue and red prints, and the image-tube plate, of the angle between the centroid of NGC 3067 and 3C 232 give -5.0° , -5.6° , and -5.5° , respectively. Therefore the angle between the QSO and the major axis of the galaxy is $\eta = 180^\circ - 101.5^\circ - 5.4^\circ = 73.1^\circ \pm 1.0^\circ$.

We also determined the central position of the galaxy by the same procedure and list it in Table II. Finally, from enlargements of the POSS blue and red prints, and the image-tube plate, we measure the projected distance from the centroid of NGC 3067 to 3C 232 as $113''.4$, $112''.8$, and $114''.2$. The calculated distance using our determination of the galaxy position and the Burbidge *et al.* (1971) QSO position is $113''.6$. We adopt the projected distance $s = 113''.5$.

REFERENCES

- Boksenberg, A., and Sargent, W. L. W. (1978). *Astrophys. J.* **220**, 42.
 Boksenberg, A., Danziger, I. J., Fosbury, R. A. E., and Goss, W. M. (1980). *Astrophys. J. Lett.* **242**, L145.
 Boksenberg, A., Snijders, M. A. J., Gull, T. R., Sargent, W. L. W., and Penston, M. V. (1981). In preparation.
 Bosma, A. (1978). Ph.D. thesis, University of Groningen, The Netherlands.
 Burbidge, E. M., Burbidge, G. R., Solomon, P. M., and Strittmatter, P. A. (1971). *Astrophys. J.* **170**, 233.
 Cowie, L. L., Songaila, A., and York, D. G. (1981). *Astrophys. J.* **246**, 653.
 Danziger, I. J., and Chromey, F. R. (1972). *Astrophys. Lett.* **10**, 99.
 de Vaucouleurs, G., de Vaucouleurs, A., and Corwin, H. G. (1976). *Second Reference Catalogue of Bright Galaxies* (University of Texas, Austin).
 Dieter, N. (1969). *Publ. Astron. Soc. Pac.* **81**, 186.
 Giovanelli, R. (1980). *Astron. J.* **85**, 1155.
 Grewing, M., and Mebold, M. (1975). *Astron. Astrophys.* **42**, 119.
 Haschick, A. D., and Burke, B. F. (1975). *Astrophys. J. Lett.* **200**, L137.
 Morgan, W. W. (1958). *Publ. Astron. Soc. Pac.* **70**, 364.
 Nilson, P. (1973). *Uppsala Obs. Ann.*, Vol. 6.
 Rubin, V. C., Ford, W. K., Jr., and Thonnard, N. (1978). *Astrophys. J. Lett.* **225**, L107.
 Rubin, V. C., Ford, W. K., Jr., and Thonnard, N. (1980). *Astrophys. J.* **238**, 471.
 Rubin, V. C., Ford, W. K., Jr., Thonnard, N., and Burstein, D. (1982). In preparation.
 Sandage, A., and Tammann, G. A. (1981). *A Revised Shapley-Ames Catalog of Bright Galaxies* (Carnegie Institution of Washington, Washington, D.C.).
 Savage, B. D., and de Boer, K. S. (1981). *Astrophys. J.* **243**, 460.
 Snijders, M. A. J. (1980). *Proceedings of the Second European IUE Conference* (ESA Scientific and Technical Publication Branch, Noordwijk, The Netherlands), Tubingen, Germany.
 Thonnard, N., Roberts, M. S., Ford, W. K. Jr., and Rubin, V. C. (1982). In preparation.